Journal of Soil Science and Plant Nutrition (2022) 22:4392–4403
https://doi.org/10.1007/s42729-022-01039-9

ORIGINAL PAPER

Base Cation Mobility in Vineyard Soils of the Colli Albani Volcanic District (Central Italy)

M. Gaeta[1] · L. Aldega[1] · M. L. Astolfi[2] · B. Bonechi[1] · P. Pacheco[3] · C. Perinelli[1,4]

Received: 18 March 2022 / Accepted: 13 October 2022 / Published online: 2 November 2022

Abstract

The quality of the Colli Albani volcanic soils has certainly contributed to the vine cultivars hence the name of one of the oldest wines (i.e., Alban wine). The alkali up to 15 wt%, $SiO2 \leq 52$ wt% and the emplacement at high temperature (≤ 600 °C) are the bedrock features that have deeply influenced the soil-forming processes in the vineyards. However, the peculiar features of the Colli Albani soils are not well known. Field survey and textural, mineralogical, and chemical data obtained with SEM, EMP, XRD, and ICP-OES were used to characterize the vineyard soils of the Colli Albani. Leucite (Lct)-bearing soils and quartz (Qz)-bearing soils occur in the studied vineyard. The Qz-bearing soils represent more weathered volcanic material, depleted in primary minerals and enriched in clays, which show a lower cation exchange capacity (CEC) than the Lct-bearing soils. CEC is a misleading definition for the Colli Albani soils because the base cation mobility in the vineyard is independent from clay mineral enrichment in the soil. Actually, the release of K, Na, Ca, and Mg depends by (i) the complete dissolution of leucite and analcime, (ii) the oxy-reaction affecting the phlogopite, which releases K + Mg, and (iii) the incongruent dissolution of clinopyroxene characterized by the "gothic texture." This texture highlights the capacity of clinopyroxene to release Ca and Mg in volcanic soils. Quantification of the texture and abundance of the primary minerals are mandatory for the management of the vineyard soils in the Colli Albani and, in general, it is significative for the vineyards in volcanic areas.

Keywords Potassic soils · Phlogopite · Clinopyroxene · Zeolites · Volcanic soils · Colli Albani · Alban wine

1 Introduction

The peri-Tyrrhenian margin of the Italian peninsula is characterized by a middle/late pleistocenic, volcanic range formed by the Colli Albani, Sabatini, Vico, and Vulsini volcanic districts from south to north, respectively. The Colli Albani volcanic district (hereafter Colli Albani) eruptive history (608–36 ka, Freda et al. 1997; Palladino et al. 2001; Marra et al. 2003; Giordano et al. 2006; Freda et al. 2006, Marra et al. 2009; Freda et al. 2011; Gaeta et al. 2011; Gaeta et al. 2016) can be divided into three main phases (Fig. 1a). The oldest (561–351 ka) was the Tuscolano-Artemisio phase (or Vulcano Laziale lithesome, Giordano et al. 2006) that consisted of several large explosive caldera-forming eruptions. The Faete phase (308–241 ka) was mainly formed by effusive, peripheral eruptions and by subordinate strombolian events, leading to the formation of a small, central edifice (i.e., Monte delle Faete, Fig. 1b) within the Tuscolano-Artemisio caldera. The youngest (201–36 ka) was the hydromagmatic phase (or Via dei Laghi lithesome, Giordano et al. 2006), which was characterized by pyroclastic-surge eruptions from tuff rings and maars (e.g., Albano maar, Fig. 1b). Huge pyroclastic-flow deposits (> 280 km^3), that mantle the surface with a volcanic cover up to 20 m thick, were emplaced during the oldest activity of Colli Albani. This cover spreads radially as far as 50 km from the vent, reaching the southeastern suburbs of the City of Rome (Marra et al. 2019). The soil quality onto the gentle slopes of the Colli Albani has certainly contributed to Ancient Rome's growth, where one million inhabitants could

✉ M. Gaeta
mario.gaeta@uniroma1.it

1 Dipartimento di Scienze della Terra, Sapienza Università di Roma, P.le Aldo Moro 5, 00185 Rome, Italy

2 Dipartimento di Chimica, Sapienza Università di Roma, P.le Aldo Moro 5, 00185 Rome, Italy

3 ÔMINA ROMANA, Via Fontana Parata, 75 - 00049 Velletri (RM), Italy

4 C.N.R-Istituto di Geologia Ambientale E Geoingegneria C/o Dipartimento di Scienze della Terra, Sapienza Università di Roma, Rome, Italy

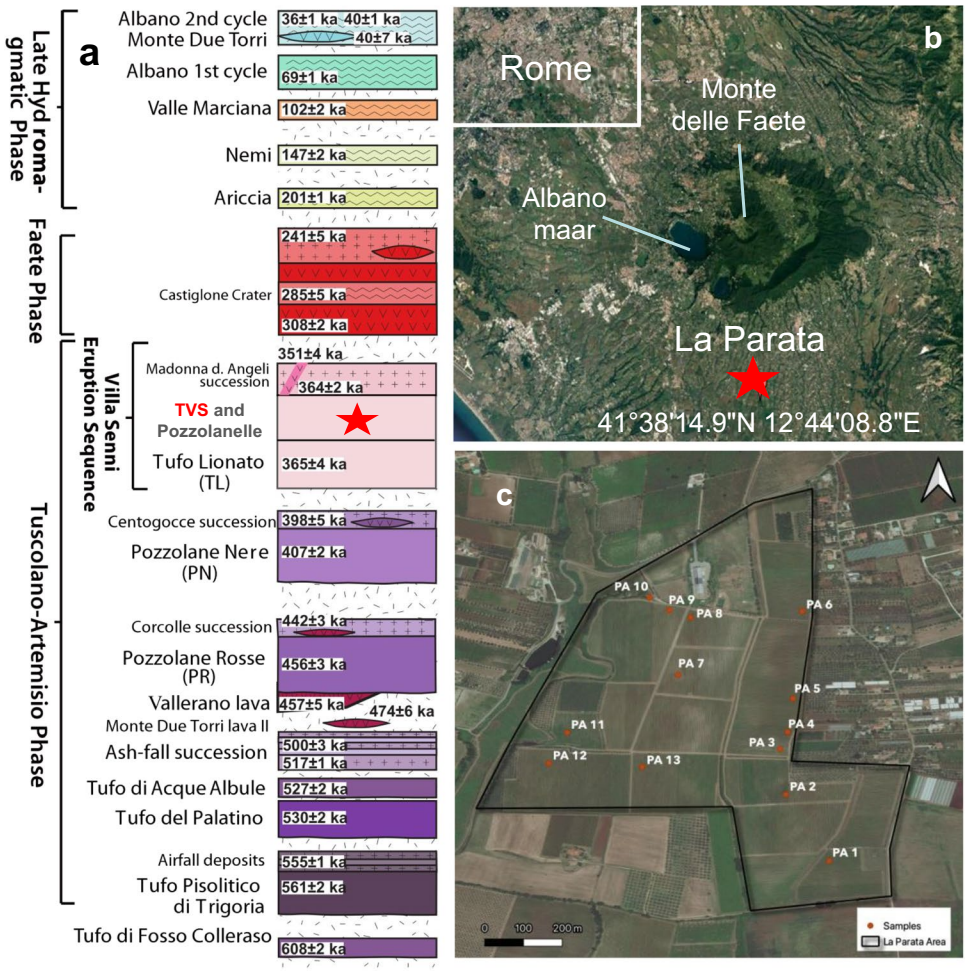

Fig. 1 Stratigraphic successions and chronological constraints available for the Colli Albani Volcanic District (**a**). Satellite image showing the geomorphology of the Colli Albani Volcanic District and the location of the La Parata locality (**b**). Location of sampling sites in the vineyard (**c**). The red star in (**a**) indicates the stratigraphic position of the bedrock in the studied vineyard

have drunk the Alban wine as early as 2000 years ago (Lill 2000). The Alban grown in the Colli Albani was one of the most ancient wines attested in Pliny's *Naturalis Historia* (77–78 AD). Interestingly, the Colli Albani soils developed on pyroclastic rocks with a peculiar K-foiditic composition (Gaeta et al. 2006, 2021; Boari et al. 2009; Fabbrizio et al. 2018) and their in-depth knowledge is essential to respond to the current and increasingly demand sustainable soil use. For example, ensuring naturally K levels in the berry, adequate to the request wine quality, is very desirable because it would reduce input and waste management costs at the winery (Mpelasoka et al. 2003). Consequently, the presence and abundance of the K-bearing, primary, and authigenic minerals should be carefully evaluated during the characterization of the vineyard soils in volcanic areas (Dahlgren et al. 2004; Sparks, 1987). The Colli Albani offers a unique opportunity to study a relatively wide area (> 1500 km^2; Freda et al. 2011) of soils developed on high K and low silica pyroclastic flow deposits that were emplaced at high temperature (up to 600 °C; Trolese et al. 2017).

Studies on the volcanic soils of Colli Albani are limited or missing while several studies have been carried out on soils developed from K-bearing pyroclastic rocks of the Vico volcanic district (Lorenzoni et al. 1995; Quantin et al. 1988). However, for their higher silica content, the coeval pyroclastic rocks of the Vico volcanic district are not directly comparable with those of Colli Albani. With the aim to increase the soil knowledge, we provide field, textural, mineralogical, and chemical data for the soils of La Parata (Fig. 1) that have been historically dedicated to the vine cultivars. Our field survey and laboratory results provide new constraints for the classification of Colli Albani soils. Moreover, we have discussed the base cation mobility that appears mainly controlled by dissolution and oxidation reactions of primary volcanic minerals rather than exchanging reactions with clay minerals.

2 Materials and Methods

La Parata locality is on the south slope of Colli Albani (Fig. 1) and is characterized by annual average temperatures of 15.5 °C, an average rainfall of around 1000/1200 mm per year and Luvic Phaeozems according to 1:250,000 map of

Lazio soils (Napoli et al. 2019). The field survey in the studied area (~1 km^2) was carried out on the basis of 13 profiles, distributed homogeneously in the vineyard (Figs. 1 and 1EA). To observe carefully the pedological features of soils, the excavation of profile has been done up to 120 cm of depth or until the pyroclastic bedrock (Fig. 1EA). Each profile was sampled at ~ 40 cm of depth for the laboratory analyses. This sampling depth, below the manipulated part of the soil and above the bedrock, ensures the representativity of soil samples being the 13 profiles relatively homogeneous. Moreover, the trench dug to facilitate the water flow in the vineyard allowed the bedrock sampling relatively near the PA10 profile (Fig. 1c). The bulk soil analyses were performed for the air-dried fine-earth fraction (< 2 mm), while the microchemical analyses of bedrock minerals were effectuated on the rock thin sections.

2.1 Basic Properties of Soils

The grain size distribution was obtained in the geotechnical laboratory of the Earth Sciences Department, Sapienza University of Rome, according to Bozzano et al. (2006) and following the ASTM (American Society for Testing and Materials) D 421–85, D 422–63, D2217-85, D 854–83 protocols. The pH was measured using a pH 510 Eutec pH-meter on a (weight of soil)/(volume of water) = 1:2.5 suspension. The organic matter was measured with the redoxometric method using the reaction with the potassium dichromate which excess was titrated with the ferrous ammonium sulfate. Loss on ignition (LOI) analyses were performed by heating the samples at 105 °C, 550 °C, and 950 °C.

2.2 Scanning Electron Microscopy and Microanalysis

Secondary electron (SE) images used to investigate textural aspects of soils were collected by scanning electron microscopy (SEM) using a FEI-quanta 400 equipped for qualitative microanalysis with an EDAX Genesis system at the Earth Sciences Department, Sapienza University of Rome (Bonechi et al 2020). Quantitative microanalyses of the bedrock minerals were carried out at the CNR-Istituto di Geologia Ambientale e Geoingegneria di Roma, with a Cameca SX50 electron microprobe equipped with five wavelength dispersive spectrometers (Gaeta et al 2000). Analyses were performed using 15 kV accelerating voltage and 15 nA beam current. As standards, we employed metals for Mn and Cr, jadeite for Na, wollastonite for Si and Ca, orthoclase for K, corundum for Al, magnetite for Fe, Rutile for Ti, periclase for Mg, and apatite for P. Counting times for all elements were 20 s on peak and 10 s on both backgrounds. Light elements (Na, K) were counted first to prevent loss by volatilization. The PAP correction method was used. Hard minerals (e.g., clinopyroxene) were analyzed using a beam diameter of 1µm whereas to minimize alkali loss during soft phases (e.g., leucite, zeolites, glass) analysis, the beam was defocused to 15 µm. In order to evaluate the accuracy of the analyses, repeated analyses of three international secondary standards (Kakanui augite, Iceladic Bir-1, and rhyolite RLS132 glasses from USGS) were made prior to any series of measurements. The mean precision from the standard value was about 1% for SiO_2, 2% for Al_2O_3, 5% for K_2O, CaO, and FeO, and 8–10% for other elements. The analytical precision (2 sigma error) is 1% for elements in the concentration range > 10 wt.% oxide, 5% for elements in the range 2–10 wt.% oxide, and better than 10% for elements in the range 0.5–2 wt.% oxide.

2.3 X-ray Diffraction (XRD)

Bedrock and soil mineral analysis, performed by means of X-ray diffraction, was conducted using a Bruker D8 Advance X-ray system equipped with Lynxeye XE-T silicon-strip detector at the Department of Earth Sciences, Sapienza University of Rome (Aldega et al 2009). The instrument was operated at 40 kV and 30 mA using CuKα radiation ($\lambda = 1.5406$ Å). Samples were run between 2 and 70° 2θ with step sizes of 0.02° 2θ while spinning the sample. Data were

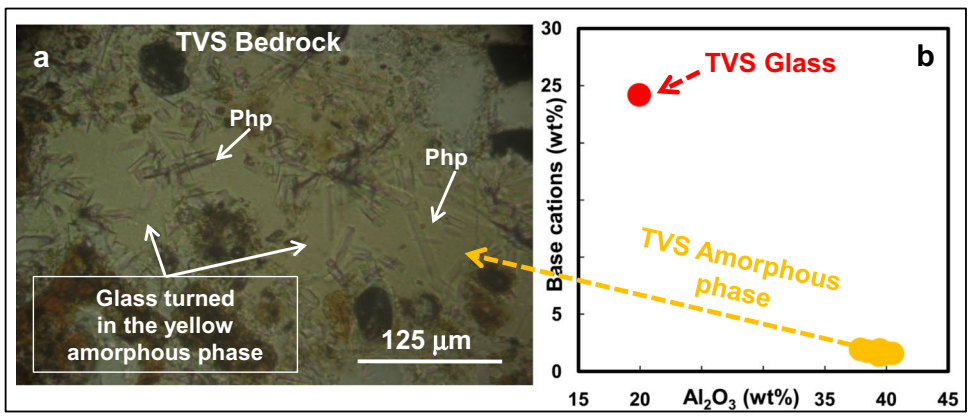

Fig. 2 Photomicrographs (plane-polarized light) of the glass in TVS bedrock matrix (**a**). The image shows that the glass is turned into pale yellow, amorphous phase including phillipsite (Php) crystals. Chemical composition of the pristine TVS glass (average of Gaeta et al. 2006 and Marra et al. 2009 data) and amorphous phase reported in the base cations vs Al_2O_3 diagram (**b**). Base cations expressed as $\Sigma K_2O+Na_2O+MgO+CaO$

collected with variable slit mode to keep the irradiated area on the sample surface constant and converted to fixed-slit mode to identify whole-powder composition.

2.4 Elemental Analysis

The total acid digestion of the soil samples was performed in a close microwave oven system (Ethos1 Touch Control; Milestone, Sorisole, Bergamo, Italy). About 0.1 g of soil was mixed with 3 mL HNO_3 69% (superpure; Carlo Erba Reagents, Milan, Italy), 1 mL HF 40% (suprapure; Merck, Darmstadt, Germany), and 1 mL HCl 30% (superpure; Carlo Erba Reagents, Milan, Italy) in a 100-mL polytetrafluoroethylene (PTFE) vessel and then heated to 180 °C with microwave energy (at a power of 1000 W) for 40 min (Astolfi et al. 2020). At the end, cooled samples were diluted to 10 mL of deionized H_2O (resistivity, ≤ 18.3 MΩ cm) from an Arioso Power I RO-UP Scholar UV system (Human Corporation, Songpa-Ku, Seoul, Korea) and filtered with syringe filters with cellulose nitrate membranes (GVS Filter Technology, Indianapolis, USA; pore size, 0.45 mm). For the leaching tests, weighed amounts (~ 0.5 g) of the soil samples were transferred into polypropylene tubes and then brought to a volume of 10 mL with deionized H_2O or 1.0 M solution of CH_3COONH_4 (Merck, Darmstadt, Germany). The tubes were then covered with a cap and left under mechanical stirring for 24 h by a rotary shaker (SB2, Cheimika, SA, Italy) at room temperature (21 °C). The extracted solutions were filtered with syringe filters with cellulose nitrate membranes and mixed with 1% HNO_3. The total and leachable contents of eight elements (Al, Ca, Fe, K, Mg, Mn, Na, and Si) were determined by inductively coupled plasma optical emission spectrometry (ICP-OES; Vista MPX CCD Simultaneous; Varian, Victoria, Mulgrave, Australia) in axial view mode and equipped with inert components (demountable torch with an alumina injector and PTFE injector holder; Sturman-Masters inert spray chamber, double pass, white Ertalyte; Agilent, Santa Clara, CA, USA) for the analysis of digests. Before the ICP-OES analysis, the digests and the extracted solutions "Ex" were diluted 1:10 with 1% HNO_3. The ICP-OES operating parameters were reported elsewhere (Astolfi et al. 2017). Calibration standards of all elements were prepared daily by diluting a single standard solution at 1000 mg/L (Merck, Darmstadt, Germany). Yttrium at 0.5 mg/L (from 1000 ± 2 mg/L; Panreac Química, Barcelona, Spain) was used as an internal standard for all measurements. The following wavelengths (nm) were used: Al 396.152, Ca 315.887, Fe 238.204, K 766.491, Mg 279.800, Mn 257.610, Na 588.995, Si 251.611, and Y 371.029. In the text, tables, and figures, the subscripts Tot, W, and Ex, refer to the element in the total solid sample, the element in the solution obtained by the leaching test with deionized water and the element in the solution obtained by the leaching test with ammonium acetate, respectively.

3 Results

3.1 Geomorphology and Basic Properties of Vineyard Soils

The 13 studied soils (Table 1) are at an elevation between 90 and 110 m above sea level and are characterized by density spanning from 1.01 to 1.35 g/cm^3, neutral pH (6.9 ± 0.8) and low organic matter content (0.70–2.55 wt%). The most widespread (9/13) soils are clayey, dark to bright brown (hue and value of the Munsell Soil Color Charts: 10YR3/3,10YR5/8) and cover the higher and flat topographic zones of the vineyard (Fig. 1, Table 1) and, in some case, rest on a gray, sandy horizon. The sandy, gray (10YR6/2) soils are present in the lower topographic zones of the vineyard characterized by relatively higher slopes and rest directly on the bedrock (Figs. 1 and 1EA). In both groups of soils, coarse fragments are scarce, and carbonate minerals are virtually absent while euhedral to subeuhedral crystals of clinopyroxene and dark mica are abundant. This highlights the origin from the underlying pyroclastic bedrock made up of the Tufo di Villa Senni (hereafter TVS; Fig. 1). The color similar to those of the bedrock (Fig. 1EA), the high content of primary minerals, including those less resistant to the weathering (i.e., leucite, analcime, and other zeolites), the coarse texture, and the absence of vertical variations indicate that four gray, sandy soils represent scarcely evolved volcanic soils or Vitric Andosols (IUSS Working Group WBR 2015). The

Table 1 Color and average values of the basic properties of soils

Sample	Color	Clay (wt%)	Silt	Sand	LOI	OM	pH	CEC (cmol(+) kg^{-1})	Soil type
PA3, PA7, PA10, PA11	Gray 10YR6/29	13 (2.5)	15 (4.3)	72 (2.1)	13.55 (0.76)	0.90 (0.23)	7.4 (0.3)	23.79 (1.30)	Lct-bearing
PA1, PA2, PA4, PA5, PA6, PA8, PA9, PA12, PA13	Dark to bright-brown 10YR3/3-10YR5/8	40 (13)	19 (4)	41 (15)	20.92 (2.06)	1.67 (0.57)	6.6 (0.4)	19.91 (1.45)	Qz-bearing

LOI, loss of ignition; *OM*, organic matter; *CEC*, cation exchange capacity; numbers out of the brackets are the averages of 4 (Lct-bearing) and 9 (Qtz-bearing) analytical measures; *()*: standard deviation

higher amount of fine fraction without evidence of eluviation horizon, the low amount of organic matter, the absence of carbonate, and the occurrence of primary clinopyroxene and dark mica indicate that the nine dark to bright-brown, clayey soils are moderately evolved volcanic soils or Vitric Cambisols (IUSS Working Group WBR 2015).

3.2 Texture, Mineral Chemistry, and Bulk Composition of the Bedrock

The TVS bedrock is a consolidated pyroclastic rock made up of submillimeter- to decimeter-sized black to purple scoria clasts and *Italites* (i.e., hypabissal, leucite-bearing rocks) enclosed within a crystal-rich matrix (Figs. 1EA and 2EA). Scoria clasts range from glassy to porphyritic (13 vol.% in the average of phenocrysts) and are sparsely vesiculated. Leucite, clinopyroxene, and dark mica, up to millimeter-sized, are ubiquitous in the scoria clasts and in the matrix (Fig. 2EA) and their abundance increases towards the top of the bedrock. Apatite, oxides, and garnet also occur (Fig. 2EA). Electron microprobe analyses (Table 2) indicate that the clinopyroxene and mica are diopsidic (i.e., $CaMgSi_2O_6$) and phlogopitic (i.e. $KMg_3AlSi_3O_{10}\bullet 2OH$) in composition, respectively, and that most of leucite (i.e., $KAlSi_2O_6$) is turned into analcime (i.e. $NaAlSi_2O_6\bullet H_2O$). The scoria clasts groundmass is made up of a microcrystalline aggregate of clinopyroxene, leucite, and other zeolites. The bedrock matrix is consolidated, made-up of zeolites ± glass (Fig. 2EA), and contains rare sanidine xenocrysts. Larger analyzable zeolites are usually chabazitic in composition (Table 2) although acicular phillipsite occurs in the matrix glass (Fig. 2a). The latter is turned into an amorphous, pale yellow phase (Fig. 2a) enriched in aluminum and depleted in the base cations with respect to the pristine composition of the TVS glass (Table 2, Fig. 2b).

3.3 Mineralogical and Chemical Composition of the Vineyard Soils

Vineyard soils show primary (i.e., those occurring in the bedrock) and authigenic minerals. Among the primary

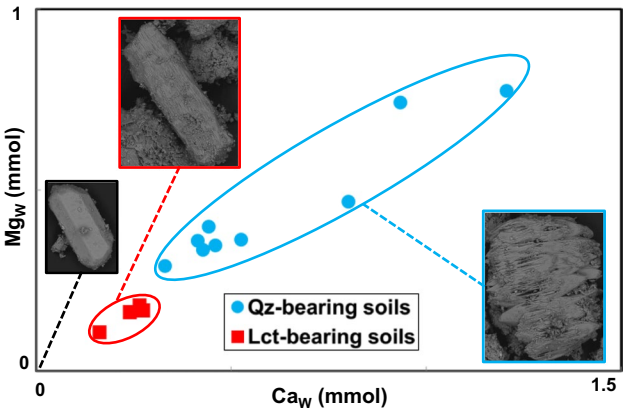

Fig. 3 Ca_W and Mg_W contents of the Lct-bearing and Qz-bearing soils. The two groups of soils show positive correlation between Ca_W and Mg_W contents. Secondary electrons (SE) images of clinopyroxenes as a function of chemical alteration intensity (increase from left to right) are also reported. In particular, clinopyroxene with gothic texture (heavenly contour) are frequent in the Qz-bearing

Table 2 Electron microprobe analyses of the minerals (single point analysis), amorphous phase (single point analysis), and pristine glasses (average composition) in the TVS bedrock

	Lct	Cpx	Phl	Anl	Cbz	Amorphous phase	Glass* [18]	σ
SiO_2	54.66	46.83	36.29	54.80	46.12	40.41	46.44	0.38
TiO_2	0.00	1.52	2.55	0.06	0.10	0.39	0.69	0.03
Al_2O_3	22.94	6.53	15.56	24.06	22.48	30.94	19.35	0.17
MgO	0.00	12.79	17.96	0.00	0.50	0.20	1.51	0.03
CaO	0.00	24.35	0.00	0.34	7.76	0.31	7.68	0.21
MnO	0.00	0.14	0.13	0.06	0.04	0.08	0.23	0.03
FeO	0.42	7.47	11.57	0.52	1.04	3.35	6.71	0.17
Na_2O	0.11	0.28	0.91	9.10	0.60	0.12	4.93	0.15
K_2O	21.05	0.04	9.73	0.06	6.35	0.58	9.37	0.25
P_2O_5	0.00	0.00	0.00	0.00	0.02	0.06	0.21	0.04
SO_3	0.00	0.02	0.00	0.00	0.11	0.09	0.42	0.07
F	0.00	0.19	0.92	0.08	0.08	0.14	0.51	0.14
Cl	0.00	0.00	0.00	0.00	0.07	0.52	0.17	0.01
Total:	99.18	100.13	95.62	89.09	85.27	77.19	98.22	

Lct, leucite; *Cpx*, clinopyroxene; *Phl*, phlogopite; *Cbz*, chabazite; *[]*, number of analyses; σ, standard deviation; *glass data after Gaeta et al 2006 and Marra et al 2009

minerals, leucite and analcime + chabazite + phillipsite (hereafter analcime and other zeolites) are observed almost exclusively in the gray sandy soils (hereafter Lct-bearing soils; Table 3). On the other hand, authigenic quartz (Fig. 3EA), albite, hematite, and mixed-layered clays occur only in the dark to bright brown clayey soils (hereafter Qz-bearing soils). K-feldspar and scarce, authigenic zeolites of the heulandite-group are present in both the Lct-bearing and Qz-bearing soils (Table 3). The pristine habit of leucite, analcime, and other zeolites is never preserved being the anhedral forms common in the Lct-bearing soils. Differently, the habit of clinopyroxenes ranges from prismatic, typical of pristine crystals, to gothic-like (Fig. 3). In particular, this unique texture develops on the crystal cleavage planes of the strongly weathered clinopyroxenes where etch pits, with walls of variable thickness (up to < 1 µm), have been formed (Figs. 4 and 4EA). Conical structures, common in Qtz-bearing soils, are another amazing characteristic of the gothic-like texture (Fig. 5a). SEM images, microanalytical and XRD data indicate that phlogopite is different in the two groups of soils. The phlogopite in the Qz-bearing soils shows a worse cleavage (Fig. 5EA), higher Fe content, and shorter distance between the (001) crystallographic planes than the phlogopite from the Lct-bearing soils (Fig. 5EA). Among the authigenic minerals, halloysite occurs in both Lct-bearing and Qz-bearing soils (Table 3, Fig. 6). However, the SEM images indicate that also halloysite has different morphology in the two types of soil. The Lct-bearing soils show fine grained, globular shape halloysite (Fig. 6a), which occurs as larger, tabular crystals in Qz-bearing soils (Fig. 6b). As stated above, the neoformation of authigenic quartz is peculiar in Qz-bearing soils where botryoidal hematite (Fig. 3EA), mixed-layered minerals, and relatively abundant alkali feldspar are also present (Table 3). In particular, a broad XRD peak at about 1.5 nm suggests the presence of random ordered mixed layered clays with smectite layers. The occurrence of smectite layers in the Qz-bearing soils is confirmed by the water loss up to ~ 100 g/kg (Table 4) at low temperature (≤ 105 °C). The Lct-bearing soils, devoid of mixed-layered minerals, have a lower water loss at T ≤ 105 °C (Table 4). The two groups of soils show a higher Si molar fraction (i.e., $(Si)_{mol}$/ $\Sigma cations_{mol}$) than the TVS bedrock (Table 4). The corresponding increase of silica activity is revealed by the crystallization of authigenic quartz and alkali feldspar in the Qz-bearing soils (Table 3). On the other hand, the lowest alkali, Ca, and Mg total contents of the Qz-bearing soils (Table 4, Fig. 5) are in agreement with the absence of leucite, analcime, and the low abundance of other zeolites and clinopyroxene (Table 3). Trends of the elements leached in laboratory with deionized water (W subscript, Table 5) point out that water chemistry of the vineyard soils is controlled by the interaction of H_2O with different mineral species. The positive correlation between Ca_W and Mg_W contents (Fig. 3) indicates that the weathered clinopyroxene releases Ca and Mg in the water circulating within the soils. The K_W *vs* Na_W opposite trends of the two groups of soils (Fig. 7a) suggest that the alkali contents of the water circulating in the Lct-bearing and Qz-bearing soils are controlled by other minerals as well. In particular, the positive correlation between K_W and Na_W contents observed in the Lct-bearing soils suggests that water chemistry in the vineyard soils is controlled by mineral phases containing both elements (i.e., leucite and analcime). On the other hand, the almost constant content of Na_W with respect to the variation of K_W observed in Qz-bearing soils (Fig. 7a) suggests that alkali are almost totally release from the phlogopite. A similar indication is obtained from the elements leached in laboratory with ammonium acetate (Ex subscript, Table 5) being the $K_{Ex} + Mg_{Ex}$ and Fe_{Ex} inversely correlated (Fig. 7b). The similar average $Alkali_{Ex}/Alkali_{Tot}$ ratio (Fig. 8) and the different contents of leucite and analcime (Table 3) confirm that the release of alkali in the soil solutions of the two groups of soils is caused from distinct primary minerals (Fig. 8). Moreover, the Qz-bearing soils show the lower content of K_{Ex}, Na_{Ex}, Ca_{Ex}, and cation exchange capacity (CEC, the ability to adsorb exchangeable cations) despite their higher clay and organic matter contents than those of Lct-bearing soils (Table 1).

4 Discussion

The studied vineyard soils show textural, mineralogical, and chemical differences despite their occurrence in a relatively restricted area characterized by the same volcanic bedrock (i.e., Tufo di Villa Senni pyroclastic flow deposit).

Table 3 Average mineralogical composition of the TVS bedrock and soils obtained with XRD

Rock/soil type	Lct	Cpx	Phl	Anl	Cbz	Php	Ap	Kfs	Qz	Alb	Hal-7	ML	Hem	Hul
TVS bedrock [2]	**	****	**	**	**	**	*	*						
Lct-bearing [4]	*	***	****	****	*	**	*	*			*			*
Qz-bearing [9]		**	**		*			**	****	*	***	*	*	*

[], number of samples; *Anl*, analcime; *Lct*, leucite; *Cpx*, clinopyroxene; *Phl*, phlogopite; *Kfs*, K-feldspar; *Php*, phillipsite; *Ap*: apatite; *Cbz,* chabazite; *Alb*, albite; *Hal-7*, halloysite-7 Å; *ML*, mixed-layered minerals; *Hem*, hematite; *Hul*, heulandite; mineral abundance: > 25 vol% (****), 25 to 15 vol% (***), 15 to 5 vol% (**), and < 5 vol % (*)

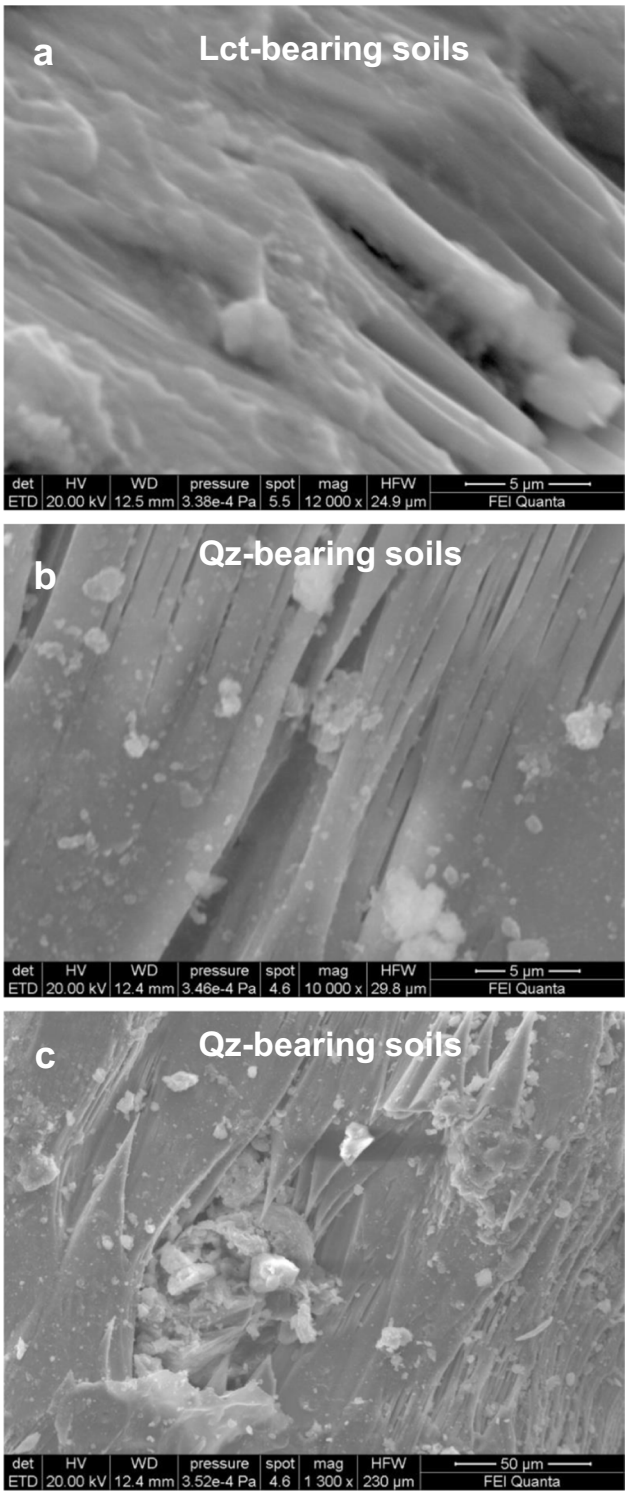

Fig. 4 Details of the "gothic" texture reported in Fig. 3 SE images showing etch pits developed on the crystal cleavage planes (**a**), walls of pits borders (**b**) with variable thickness (up to 1µm) and gothic texture (**c**)

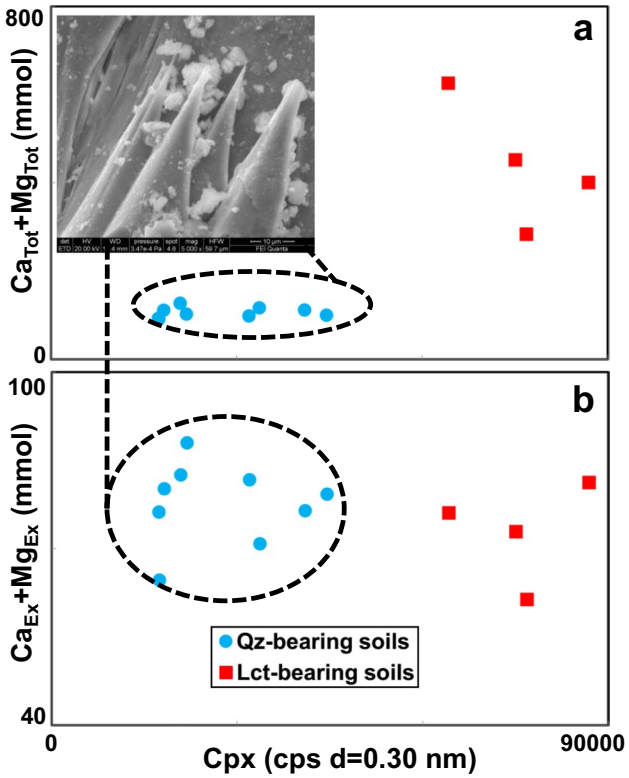

Fig. 5 Ca_{Tot}+ Mg_{Tot} (**a**) and Ca_{Ex} + Mg_{Ex} (**b**) contents of the Lct-bearing and Qz-bearing soils. Cation contents are plotted versus the abundance of clinopyroxene expressed as counts per second (CPS) of the X ray diffraction peak at d=0.30 nm. The clinopyroxene is less abundant in the Qz-bearing soils but is more intensely weathered as indicated by the conical structures (SE image) developed in the gothic texture

In particular, the bedrock is formed by pyroclastic rocks originating from magmas characterized by high K_2O (~9 wt%) and CaO (~8 wt%) and low SiO_2 (~46 wt%) contents. This magma composition favors the crystallization of the two main minerals of the Colli Albani volcanic rocks: the leucite and clinopyroxene diopsidic in composition. Pristine clinopyroxene is common in both lavas and pyroclastic rocks of Colli Albani. Differently, pristine leucite is relatively scarce in the rocks deriving from high temperature (up to ~600 °C; Trolese et al. 2017), pyroclastic flow deposit because leucite to analcime conversion is a fast reaction (i.e., a few days at temperatures between 150 and 300 °C) with low activation energy (Gupta and Fyfe 1975; Putnis et al. 2007). Consequently, in the cooling and degassing stage of the TVS bedrock, a large part of the leucite is turned into analcime, and the matrix glass is turned in chabazite, phillipsite, and Al-rich amorphous phase by similar reactions. However, pristine glasses are rare in the Colli Albani volcanic rocks (Gaeta 1998) also for the low viscosity of K-foiditic magmas that increase the crystal growth rate and hamper glass formation (Bonechi et al. 2020; Gaeta et al. 2021).

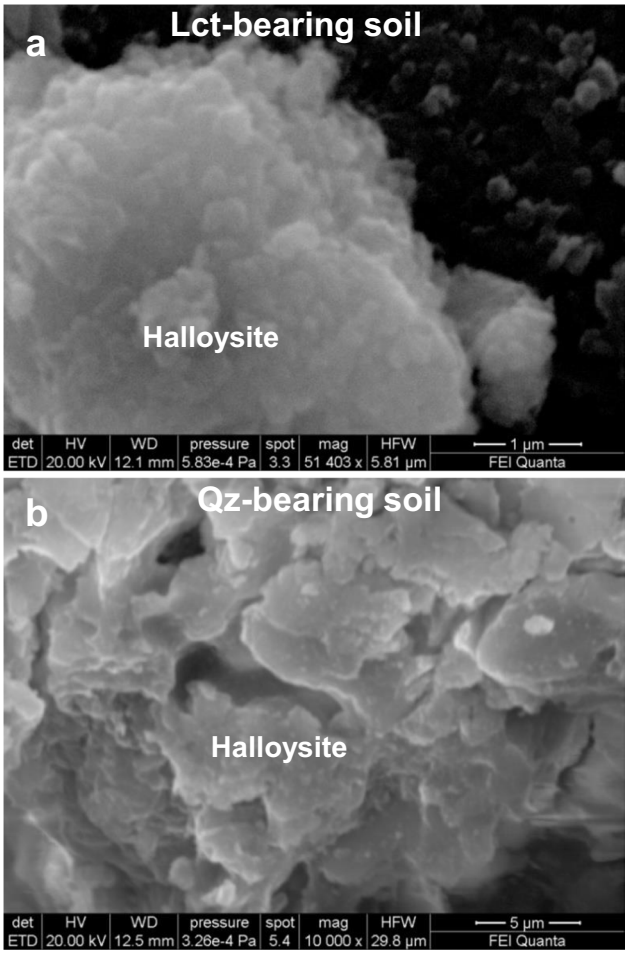

Fig. 6 SE images of fine grained, globular of halloysite in the Lct-bearing soil (**a**) and tabular halloysite in the Qz-bearing soil (**b**)

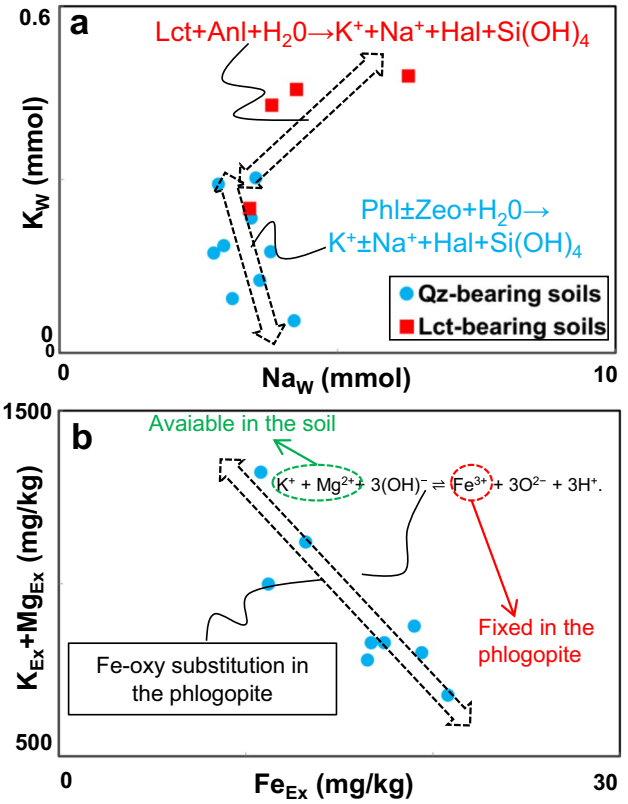

Fig. 7 K_W and Na_W contents of the Lct-bearing and Qz-bearing soils. The Lct-bearing soils show positive correlation between K_W and Na_W contents due to the dissolution of leucite and analcime. The Qz-bearing soils, differently, show only the variation of K_W caused by the chemical alteration of phlogopite (**a**). Abundance of the potassium, magnesium and iron obtained from the Qz-bearing soils leached with the ammonium acetate. The correlation between K_{Ex} + Mg_{Ex} and Fe_{Ex} in the Qz-bearing soils supports the Fe-oxy substitution reaction in the phlogopite (see text) that releases magnesium and potassium in the soils and fixes the iron in the mica (**b**)

The compositional and mineralogical peculiarities of the TVS bedrock control the abundance of leucite, analcime (± other zeolites), clinopyroxene, and phlogopite crystals in the vineyard soils. The Lct-bearing soils, similarly to the Vitric Andosols, are weakly developed volcanic soils dominated by primary minerals. These soils rest on the TVS bedrock and occur in a morphological position that favors the erosion of the higher part of the profile. The thick (> 2 m) soil profiles of the vineyard should be formed by a superficial, more weathered horizon (cambic), with features similar those of Qtz-bearing soils, that rests above a horizon (C) resembling the Lct-bearing soils. The latter are immature volcanic soils that, however, show a higher CEC than the Qz-bearing soils. Starting from this framework, the pedogenetic processes and base cation mobility in the vineyard soils will be discussed in the following.

The occurrence and/or abundance of glasses cannot be used to discriminate the evolutionary stage of the Colli Albani soils. More useful appears the conservation of soft primary minerals (leucite, analcime, and other zeolites) or the crystallization of authigenic quartz. The occurrence of quartz in superficial horizons of thick soils of the Colli Albani was previously reported by Marra et al. (2019) that excluded an eolian-origin. The elongated shape of quartz is entirely convincing of a non-eolian origin and it is unrealistic, on the other hand, to image that eolian quartz choses to deposit only in the clayey soils without leucite and analcime. This information on the origin of quartz in the Colli Albani soils is of great significate for future researches focused on the traceability of high-quality wines on the basis of isotope ratios (Tescione et al 2020).

The Lct-bearing soils occur at lower topographic levels than the Qz-bearing soils and in multi horizons profiles are below the Qz-bearing soils. The enrichment in the fine-grained clasts, the occurrence of authigenic quartz, swelling minerals, and hematite, the decrease of primary minerals, and their location atop the Lct-bearing soils indicate that Qz-bearing soils represent more weathered volcanic material and derive from the Lct-bearing soils. Pedogenetic processes leading to the formation of the Qz-bearing soils

Table 4 Averages (g kg^{-1}) of Si_{Tot}/Al_{Tot} ratio, silica molar fraction (X_{Si}), Σ of base cation abundance and water loss at various T°C

Rock/soil type	Si_{Tot}/Al_{Tot}	X_{Si}	$(Ca+Mg+K+Na)_{Tot}$	105 °C	550 °C	950 °C
TVS bedrock [2]	2.3	0.47	142	18.5	44.6	7.0
Lct-bearing [4]	2.1 (0.4)	0.55 (0.03)	45 (8)	36.9 (5.7)	90.3 (2.4)	8.4 (2.6)
Qz-bearing [9]	1.7 (0.3)	0.53 (0.03)	13 (3)	77.4 (19.9)	120.6 (9.1)	11.3 (2.3)

[], number of samples; *()*, standard deviation

Table 5 Averages of cations (mg kg^{-1}) extracted from soils using deionized water ($cation_W$) and ammonium acetate ($cation_{Ex}$)

Soil type	Si_W	Al_W	Fe_W	Mg_W	Ca_W	Na_W	K_W	Fe_{Ex}	Mg_{Ex}	Ca_{Ex}	Na_{Ex}	K_{Ex}
Lct-bearing [4]	301 (27)	142 (24)	46 (9)	4 (1)	10 (2)	102 (29)	16 (4)	7 (1)	433 (146)	2207 (253)	1013 (314)	1847 (617)
Qz-bearing [9]	239 (96)	114 (71)	45 (27)	11 (4)	25 (12)	77 (11)	7 (3)	16 (4)	609 (131)	2112 (179)	304 (328)	306 (264)

[], number of samples; *()*, standard deviation

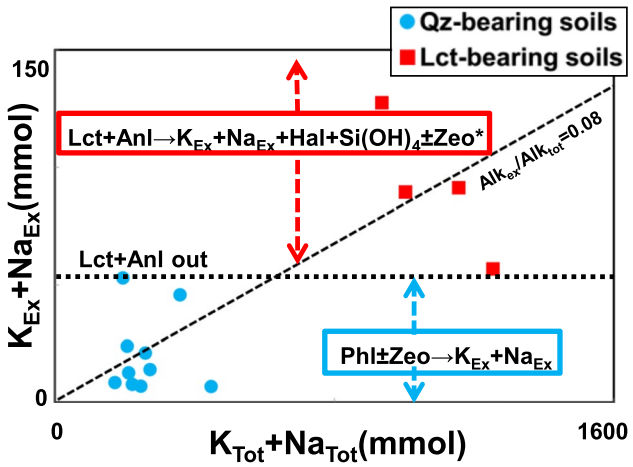

Fig. 8 $Alkali_{Ex}$ and $Alkali_{Tot}$ contents of the Lct-bearing and Qz-bearing soils. The average $Alkali_{Ex}/Alkali_{Tot}$ ratio (~0.08) of the two groups of soils is similar and it is indicated by the dashed line. The higher amount of the K_{Ex} and Na_{Ex} measured in the Lct-bearing soils is due to the dissolution of leucite and analcime. Phlogopite and zeolites are the main source for K_{Ex} and Na_{Ex} in the Qz-bearing soils. Lct: leucite; Phl: phlogopite; Alb: albite; Zeo*: authigenic zeolites

are conditioned by the sandy texture and low organic matter content of the Lct-bearing soils that have, consequently, high permeability and pH≈7. In these conditions, highly soluble minerals such leucite and analcime readily disappear from the soils (Wilkin and Barnes 1998). The dominant solubility-controlling reactions of leucite and analcime in the Lct-bearing soils are:

$$KAlSi_2O_6(Lct) + 6H_2O \leftrightarrow K^+ + Al(OH)_{4^-} + 2Si(OH)_4(aq) \quad (1)$$

$$NaAlSi_2O_6 \cdot H_2O(Anl) + 5H_2O \leftrightarrow Na^+ + Al(OH)_{4^-} + 2Si(OH)_4(aq) \quad (2)$$

where Lct is leucite; Anl, analcime; and aq, aqueous species.

In the Lct-bearing soils, both solubility reactions are shifted to the right because at pH≈7, the $Al(OH)_4^-$ activity in aqueous solutions is negligible (Dahlgren et al. 2004). The net result of these solubility reactions is the incipient crystallization of fine grained halloysite with globular shape in the Lct-bearing soils. In particular, halloysite crystallization is promoted by (i) the high permeability that allows the rapid transport of K^+ and Na^+ away from the mineral–water interface and (ii) the precipitation of Al and silica catalyzed by the Al-rich, amorphous phase that derives from the TVS bedrock. The Si_{Tot}/Al_{Tot} ≈2 measured in Lct-bearing soils indicates that the excess of silica, due to the disproportion between the aqueous Al and Si species (Si/Al = 2) and the precipitated Al and Si as halloysite (Si/Al = 1), should be buffered by the reprecipitation of silica-rich minerals. Actually, the XRD analysis shows K-felspar and evidence of heulandite-group zeolites, which have higher silica content than the analcime (Wilkin and Barnes 1998).

Clinopyroxene weathering takes place, causing the enlargement and coalescence of etch pits developed on crystal dislocations with the formation of the unique "gothic" texture. This texture results from the leaching of Ca and Mg ± Fe and the passive accumulation of Al and Si on the walls and inside the etch pits. Actually, the positive correlation between Ca_W and Mg_W contents indicates that the weathered clinopyroxene releases Ca and Mg in the water circulating within the soils. On the other hand, the tips of conical structures and the micrometric fragments in the etch pits show a halloysite-like composition. The Mg and Ca total contents are higher in the Lct-bearing than in the Qz.-bearing soils, in agreement with the clinopyroxene abundance estimated for the two groups of soils. Differently, the Mg_{Ex} and Ca_{Ex} and the Mg_W and Ca_W contents measured in the Qz-bearing soils are respectively similar and higher than those measured in the Lct-bearing soils. The data on the Mg and Ca leached in the laboratory indicate a large number of sites where Mg and Ca can be removed despite the lower clinopyroxene abundance in the Qz-bearing soils. The more efficient protonation in

the Qz-bearing soils causes, indeed, the stronger dissolution of clinopyroxene testified by the conical structures. Moreover, the Mg_W/Ca_W atomic ratio < 1 indicates that Fe is released from the weathered clinopyroxene together with Mg. Clinopyroxene and phlogopite in the bedrock are, indeed, abundant and relatively Fe-rich (FeO_{Tot} up to ~ 12 wt%), and their contribution to the Fe enrichment in soils is certainly higher than that of Ti-magnetite, whose abundance is low in the bedrock (< 1 vol%).

The phlogopite in the Qz-bearing soils has a lower basal spacing than that observed for the phlogopite occurring in Lct-bearing soils and TVS bedrock. The decrease of the basal spacing in the phlogopite cannot be explained by the replacement of K with hydrated exchangeable cations. This process, indeed, should lead to an increase in the phlogopite basal spacing. Nevertheless, the relatively high K_{Ex} content in the Qz-bearing soils is certainly due to phlogopite leaching because leucite and analcime are absent and the other zeolites are scarce. The increase of Fe in phlogopite and the $K_{Ex} + Mg_{Ex}$ vs Fe_{Ex} correlation observed in the Qz-bearing soils indicate that the Fe-oxy substitution reaction [3] causes the shortening of the interlayer distance along the c-axis,

$$K^+ + Mg^{2+} + 3(OH)^- \rightleftharpoons Fe^{3+} + 3O^{2-} + 3H^+ \quad (3)$$

releases K and Mg in the water soil and immobilizes the Fe in phlogopite. XRD data and the water loss up to ~ 10 wt% at the lowest temperature indicate the presence of expandable mixed-layered minerals in the Qz-bearing soils (Velde 1985). This kind of mixed layering has been observed in similar phlogopite-bearing deposits affected by chemical alteration in the karst environment (Aldega et al. 2009). The formation of smectite layers interlayered with phlogopite is favored by the increase of Mg and Ca activities in the soil water caused by the chemical alteration of the clinopyroxene in the Qz-bearing soils. Actually, the Qz-bearing soils, which are characterized by lower Ca and Mg total contents than the Lct-bearing soils, show higher Ca_W and Mg_W contents according to a more intense weathering stage of clinopyroxene. The more efficient protonation in the Qz-bearing soils, due to the decrease of pH, causes the complete dissolution of clinopyroxene and the release of Ca, Mg, Al, and silica in the soil water. The sudden increase of the Ca, Mg, Al, and silica activities in the water, coupled with the limited ionic mobility within the clay-rich soils, yields in the crystallization of expandable mixed-layered minerals. Nevertheless, halloysite is the most abundant clay mineral formed during the progressive weathering of the vineyard soils as documented by abundant, large, tabular halloysite crystals that are present in the Qz-bearing soils. Additionally, the low amount of organic matter, the redox conditions (i.e., $E_h \geq 0$ v), and the Fe fixation in the phlogopite favor the crystallization of authigenic hematite in the Qz-bearing soils. The crystallization of hematite and the exhaustion of reactions [1] and [2] yield a slight pH decrease (~ one pH unit). This more acidic environment accelerates the protonation of the weathered clinopyroxene that becomes the main source of silica. The disproportion between the aqueous Al and Si species released from the clinopyroxene (Si/Al≈3) and the Al and Si precipitated as halloysite (Si/Al = 1) is buffered (i.e., $Si_{Tot}/Al_{Tot} \approx 2$) by the neoformation of quartz and alkali feldspar in the Qz-bearing soils.

The positive correlation between Ca_W and Mg_W contents, in the absence of other Ca-Mg-bearing minerals (e.g., dolomite), indicates that the weathered clinopyroxene releases Ca and Mg in the water soils. Moreover, the lack of correlation between $Mg_{Tot} + Ca_{Tot}$ and $Mg_{Ex} + Ca_{Ex}$ contents and the clinopyroxene abundance suggest differences in the releasing processes for the two groups of soils. SEM images show that the chemical alteration of the clinopyroxene is mediated by the specific surface whose intensity increases from the Lct-bearing to Qz-bearing soils. The etch pits in the Lct-bearing soils are the source of Ca and Mg ± Fe and the trap for Al and silica. Thus, the contribution of clinopyroxene to the Ca and Mg mobility should be considered like an incongruent dissolution process in the Lct-bearing soils. Differently, the chemical alteration of clinopyroxene in the Qz-bearing soils is likely a total dissolution process in a partially closed-system where the mobility of Ca and Mg is limited by the relatively low permeability due to the clayey texture and crystallization of small amounts of expandable mixed-layered minerals. The Mg mobility is also controlled by the chemical alteration of phlogopite through reaction [3] that releases the K and Mg in the soil water and fixes the Fe. The Fe-oxy reaction [3] is function of the Eh that, in turn, is mainly controlled by organic matter in the soil. Consequently, the low amount of organic matter favoring the high O_2 activity in the soil is the intrinsic factor that enhances the K availability in the Qz-bearing soils. Average $Alkali_{Ex}/Alkali_{Tot}$ ratio of the two groups of soils is similar, although, the alkali-bearing minerals, their stability, and reactions of alkali releases are different. The high amount of the K_{Ex} and Na_{Ex} measured in the Lct-bearing soils depends on the presence of highly soluble leucite and analcime. The pH≈7 of the Lct-bearing soils promotes the release of alkali in soil water through reactions [1] and [2] that are pH-controlled because involving hydro metal ions (e.g., $Al(OH)_n$). In particular, the contribution of leucite and analcime to the base cations mobility should be considered an open-system solubility process. If reprecipitation of authigenic zeolites is excluded in this system, the parameter that controls leucite and analcime solubility, besides the pH, is the solvent flux.

The Lct-bearing soils are an intriguingly case study of high alkali contents in weakly developed volcanic soils. Ensuring base cation levels in the soils adequate to the vineyards sustainability and request wine quality is mandatory

in the modern wine farms (Mpelasoka et al. 2003). The leaching is the main natural process that can decrease the alkali concentration in the Lct-bearing soils characterized by highly soluble leucite and analcime. The irrigation, enhancing the solvent flux, could be able to remove undesirable alkali excess occurring in these soils. The dissolution of leucite and analcime is a relatively rapid process, nevertheless, the high permeability of Lct-bearing soils limits, for the absence of cohesive forces, the formation of water solutions in contact with the primary minerals. The reduction of the alkali concentration caused by the irrigation was observed, indeed, in the clayey soils (Dundon and Smart 1984; Klein et al. 2000). As stated above, in addition to the solvent flux, the main factor that can increase the alkali leaching rate in the Lct-bearing soils is the pH decrease of the soil water. In soils with low amount of organic matter, as the Lct-bearing soils, or where addition of manures or crop residues is not practiced, the pH of soil water is destined to remain neutral. Interestingly, where symbiotic N fixation occurs, it has been observed that nitric acid generated during nitrification led to high rates of NO_3-driven cation leaching (Homann et al. 1992).

5 Conclusion

The vineyard soils in the Colli Albani volcanic district were developed on pyroclastic flow deposits that are characterized by high K and low silica contents and by an emplacement temperature of about 600 °C. These primary chemical and physical features are responsible for ab initio properties that have deeply influenced the final composition of soils. Morphological, textural, mineralogical, and chemical data indicate that the evolutionary stages of the Colli Albani soils consist in TVS bedrock → Lct-bearing soils → Qz-bearing soils. Interestingly, less developed Lct-bearing soils in the vineyard show a higher cation exchange capacity than that observed for the more developed Qtz-bearing soils. Data reported and discussed indicate, indeed, that the base cation mobility is controlled by the abundance and speciation of the primary volcanic minerals rather than authigenic clay minerals. In particular, the reactions that control the abundance of base cations in soil solutions are as follows: (i) the dissolution of leucite, analcime, and other zeolites, in the less developed volcanic soils; (ii) the incongruent and/or specific site dissolution of clinopyroxene, in both type of soils, and (iii) the oxy-reaction affecting the phlogopite, in the more developed volcanic soils. The quantification of these reactions, that are relatively uncommon among pedogenetic processes, is mandatory for the management of the vineyard soils and, in general, for the quality conservation of Colli Albani soils.

Supplementary Information The online version contains supplementary material available at https://doi.org/10.1007/s42729-022-01039-9.

Acknowledgements We thank T. Ruspandini (Sapienza, Università di Roma) and M. Serracino (CNR-IGAG) for their assistance during SEM and EPMA analytical sessions, D. Mannetta (Sapienza, Università di Roma) for the realization of the rock thin sections, and I. Palermo for drawing the figures. MG is also grateful to S. Minutillo Turtur who introduced him to the OMINA.

Funding Open access funding provided by Università degli Studi di Roma La Sapienza within the CRUI-CARE Agreement.

Declarations

Conflict of Interest The authors declare no competing interests.

References

Aldega L, Cuadros J, Laurora A, Rossi A (2009) Weathering of phlogopite to beidellite in a karstic environment. Am J Sci 309:689–710. https://doi.org/10.2475/08.2009.03

Astolfi ML, Di Filippo P, Gentili A, Canepari S (2017) Semiautomatic sequential extraction of polycyclic aromatic hydrocarbons and elemental bio-accessible fraction by accelerated solvent extraction on a single particulate matter sample. Talanta 174:838–844. https://doi.org/10.1016/j.talanta.2017.06.072

Astolfi ML, Protano C, Marconi E, Massimi L, Brunori M, Piamonti D, Migliara G, Vitali M, Canepari S (2020) A new treatment of human hair for elemental determination by inductively coupled mass spectrometry. Anal Methods-UK 12:1906–1918. https://doi.org/10.1039/C9AY01871A

Boari E, Avanzinelli R, Melluso L, Giordano G, Mattei M, De Benedetti AA, Morra V, Conticelli S (2009) Isotope geochemistry (Sr–Nd–Pb) and petrogenesis of leucite-bearing volcanic rocks from "Colli Albani" volcano, Roman Magmatic Province, Central Italy: inferences on volcano evolution and magma genesis. Bull Volcanol 71:977–1005. https://doi.org/10.1007/s00445-009-0278-6

Bonechi B, Perinelli C, Gaeta M (2020) Clinopyroxene growth rates at high pressure: constraints on magma recharge of the deep reservoir of the Campi Flegrei Volcanic District (south Italy). B Volcanol 82:5. https://doi.org/10.1007/s00445-019-1342-5

Bozzano F, Gaeta M, Marcoccia S (2006) Weathering of Valle Ricca stiff and jointed clay. Eng Geol 84:161–182. https://doi.org/10.1016/j.enggeo.2005.11.010

Dahlgren RA, Saigusa M, Ugolini FC (2004) The nature, properties and management of volcanic soils. Adv Agron 82:113–182

Dundon CG, Smart RE (1984) Effects of water relations on the potassium status of Shiraz vines. Am J Enol Viticult 35:40–45
Fabbrizio A, Gaeta M, Carroll MR, Petrelli M (2018) Crystallization induced Sulfur and REE zoning in apatite: the example of the Colli Albani's magmatic system. Eur J Mineral 125–133. https://doi.org/10.1127/ejm/2018/0030-2701
Freda C, Gaeta M, Palladino DM, Trigila R (1997) The Villa Senni Eruption (Alban Hills, central Italy): the role of H_2O and CO_2 on the magma chamber evolution and on the eruptive scenario. J Volcanol Geoth Res 78:103–120. https://doi.org/10.1016/S0377-0273(97)00007-3
Freda C, Gaeta M, Karner DB, Marra F, Renne PR, Taddeucci J, Scarlato P, Christensen JN, Dallai L (2006) Eruptive history and petrologic evolution of the Albano multiple Maar (Alban Hills, Central Italy). B Volcanol 68:567–591. https://doi.org/10.1007/s00445-005-0033-6
Freda C, Gaeta M, Giaccio B, Marra F, Palladino DM, Scarlato P, Sottili G (2011) CO2-driven large mafic explosive eruptions: the Pozzolane Rosse case study from the Colli Albani Volcanic District (Italy). B Volcanol 73:241–256. https://doi.org/10.1007/s00445-010-0406-3
Gaeta M (1998) Petrogenetic implications of Ba-sanidine in the Lionato Tuff (Colli Albani Volcanic District, Central Italy). Mineral Mag 62:697–701. https://doi.org/10.1180/002646198547927
Gaeta M, Fabrizio G, Cavarretta G (2000) F-phlogopites in the Alban Hills Volcanic District (Central Italy): indications regarding the role of volatiles in magmatic crystallisation. J Volcanol Geoth Res 99:179–193. https://doi.org/10.1016/S0377-0273(00)00172-4
Gaeta M, Freda C, Christensen JN, Dallai L, Marra F, Karner DB, Scarlato P (2006) Time-dependent geochemistry of clinopyroxene from the Alban Hills (Central Italy): clues to the source and evolution of ultrapotassic magmas. Lithos 86:330–346. https://doi.org/10.1016/j.lithos.2005.05.010
Gaeta M, Freda C, Marra F, Di Rocco T, Gozzi F, Arienzo I, Giaccio B, Scarlato P (2011) Petrology of the most recent ultrapotassic magmas from the Roman Province (Central Italy). Lithos 127:298–308. https://doi.org/10.1016/j.lithos.2011.08.006
Gaeta M, Freda C, Marra F, Arienzo I, Gozzi F, Jicha B, Di Rocco T (2016) Paleozoic metasomatism at the origin of Mediterranean ultrapotassic magmas: constraints from time-dependent geochemistry of Colli Albani volcanic products (Central Italy). Lithos 244:151–164. https://doi.org/10.1016/j.lithos.2015.11.034
Gaeta M, Bonechi B, Marra F, Perinelli C (2021) Uncommon K-foiditic magmas: the case study of Tufo del Palatino (Colli Albani Volcanic District, Italy). Lithos 396–397(106):239. https://doi.org/10.1016/j.lithos.2021.106239
Giordano G, De Benedetti AA, Diana A, Diano G, Gaudioso F, Marasco F, Miceli M, Mollo S, Cas RAF, Funiciello R (2006) The Colli Albani mafic caldera (Roma, Italy): stratigraphy, structure and petrology. J Volcanol Geoth Res 155:49–80. https://doi.org/10.1016/j.jvolgeores.2006.02.009
Gupta AK, Fyfe WS (1975) Leucite survival: the alteration to analcime. Can Mineral 13:361–363
Homann PS, van Miegroet H, Cole DW, Wolfe GV (1992) Cation distribution, cycling, and removal from mineral soil in Douglas-fir and red alder forests. Biogeochemistry 16:121–150. https://doi.org/10.1007/BF00002828
IUSS Working Group WBR (2015) World reference base for soil resources, in World Soil Resources Reports No. 106 (FAO, Rome, 2014).
Klein I, Strime M, Fanberstein L, Mani Y (2000) Irrigation and fertigation effects on phosphorus and potassium nutrition of wine grapes. Vitis 39:55–62. https://doi.org/10.5073/vitis.2000.39.55-62
Lill A (2000) Wine and a trial of character in Horace's poems. J Wine Res 11:35–57. https://doi.org/10.1080/713684205
Lorenzoni P, Mirabella A, Bidini D, Lulli L (1995) Soil genesis on trachytic and leucititic lavas of Cimini volcanic complex (Latium, Italy). Geoderma 68:79–99. https://doi.org/10.1016/0016-7061(95)00027-L
Marra F, Freda C, Scarlato P, Taddeucci J, Karner DB, Renne P, Gaeta M, Palladino DM, Trigila R, Cavarretta G (2003) Post-caldera activity in the Alban Hills volcanic district (Italy): 40Ar/39Ar geochronology and insights into magma evolution. B Volcanol 65:227–247. https://doi.org/10.1007/s00445-002-0255-9
Marra F, Karner DB, Freda C, Gaeta M, Renne P (2009) Large mafic eruptions at Alban Hills Volcanic District (Central Italy): chronostratigraphy, petrography and eruptive behavior. J Volcanol Geoth Res 179:217–232. https://doi.org/10.1016/j.jvolgeores.2008.11.009
Marra F, Gaeta M, Jicha BR, Nicosia C, Tolomei C, Ceruleo P, Florindo F, Gatta M, La Rosa M, Rolfo MF (2019) MIS 9 to MIS 5 terraces along the Tyrrhenian Sea coast of Latium (central Italy): assessing interplay between sea level oscillations and tectonic movements. Geomorphology 346.https://doi.org/10.1016/j.geomorph.2019.106843
Mpelasoka BS, Schachtman DP, Treeby MT, Thomasa MR (2003) A review of potassium nutrition in grapevines with special emphasis on berry accumulation. Aust J Grape Wine R 9:154–168. https://doi.org/10.1111/j.1755-0238.2003.tb00265.x
Napoli R, Paolanti M, Rivieccio R, Di Ferdinando S (2019) Carta dei suoli del Lazio scala 1:250000. S.E.L.C.A. Firenze.
Palladino DM, Gaeta M, Marra F (2001) A large K-foiditic hydromagmatic eruption from the early activity of the Alban Hills Volcanic District, Italy. B Volcanol 63:345–359. https://doi.org/10.1007/s004450100150
Putnis CV, Geisler T, Schmid-Beurmann P, Stephan T, Giampaolo C (2007) An experimental study of the replacement of leucite by analcime. Am Mineral 92:19–26. https://doi.org/10.2138/am.2007.2249
Quantin P, Gautheyrou J, Lorenzoni P (1988) Halloysite formation through in situ weathering of volcanic glass from trachytic pumices, Vico's Volcano, Italy. Clay Miner 23:423–437. https://doi.org/10.1180/claymin.1988.023.4.09
Sparks DL (1987) Potassium dynamics in soils. Adv Soil S 6:1–63
Tescione I, Casalini M, Marchionni S, Braschi E, Mattei M, Conticelli S (2020) Conservation of 87Sr/86Sr during wine-making of white wines: a geochemical fingerprint of geographical provenance and quality production. Front Environ Sci 8:153. https://doi.org/10.3389/fenvs.2020.00153
Trolese M, Giordano G, Cifelli F, Winkler A, Mattei M (2017) Forced transport of thermal energy in magmatic and phreatomagmatic large volume ignimbrites: paleomagnetic evidence from the Colli Albani volcano, Italy. Earth Planet Sc Lett 478:179–191. https://doi.org/10.1016/j.epsl.2017.09.004
Velde B (1985) Clay minerals: a physico-chemical explanation of their occurrence. Elsevier, Amsterdam
Wilkin RT, Barnes HL (1998) Solubility and stability of zeolites in aqueous solution: I. Analcime, Na-, and K-clinoptilolite. Am Mineral 83:46–761. https://doi.org/10.2138/am-1998-7-807